Journal of Photochemistry & Photobiology, B: Biology 211 (2020) 111994

Contents lists available at ScienceDirect

Journal of Photochemistry & Photobiology, B: Biology

journal homepage: www.elsevier.com/locate/jphotobiol

Circadian movement behaviours and metabolism differences of the Pacific abalone *Haliotis discus hannai*

Xiaolong Gao[a,b,c], Xuan Luo[a,b,c], Weiwei You[a,b,c,*], Caihuan Ke[a,b,c,*]

[a] State Key Laboratory of Marine Environmental Science, Xiamen University, Xiamen, China
[b] Fujian Key Laboratory of Genetics and Breeding of Marine Organisms, Xiamen University, Xiamen 361102, China
[c] College of Ocean and Earth Sciences, Xiamen University, Xiamen, China

ARTICLE INFO

Keywords:
Circadian rhythm
Haliotis discus hannai
Movement behaviour
Physiological metabolism

ABSTRACT

Circadian rhythm is the most important and universal biological rhythm in marine organisms. In this research, the movement behaviour of abalone (*Haliotis discus hannai*) was continuously monitored under a light cycle of 12 L:12D. It was found that the cumulative movement distance and cumulative movement time of abalone reached was highest from 00:00–03:00 h. The minimum values of maximum movement velocity occurred between 21:00–00:00 h, and a significant circadian cosine rhythm was exhibited during these periods ($P < 0.05$). Metabolomic analysis of cerebral ganglions of abalone was conducted at 06:00 h (6 M), 14:00 h (14 M), and 22:00 h (22 M) and 380, 385, and 315 metabolites with significant differences were identified in 6 M vs 14 M, 14 M vs 22 M, and 6 M vs 22 M, respectively ($P < 0.05$). With the alternation of day and night, the expression levels of phosphatidylcholine, 5-HT, *N*-acetyl-5-hydroxytryptamine, indole-3-acetaldehyde, hypoxanthine, and deoxyinosine declined significantly, while those of Lysophosphatidylcholines (lysoPC) (20: 5 (5Z, 8Z, 11Z, 14Z, 17Z)), lysoPC (22: 4 (7Z, 10Z, 13Z, 16Z)), lysoPC (16: 1 (9Z) / 0: 0), phosphatidylethanolamine (PE) (18: 1 (11Z) 22: 2 (13Z, 16Z)), and guanosine 5′-phosphate rose significantly. These 11 metabolites can be used as differential metabolic markers. These findings not only quantitatively describe the circadian movement behaviours of abalone, but also provide an initial analysis of the circadian mechanism of the physiological metabolic conversion of abalone, which in turn provides guidelines for light control and feeding strategy for use in aquaculture production.

1. Introduction

Light environment is generally considered as a complex, variable and important ecological factor [1,2]. As recognized zeitgebers, light, temperature and magnetic field can induce resetting and changes of circadian rhythm, and organisms can perceive the signal transmitted from a zeitgeber and make a change [3–5]. However, compared with other environmental factors, light cycle and temperature can provide animals with a steady seasonal rhythm, which is considered essential for the normal physiological development of aquatic organisms [6].

In nature, almost all living organisms, ranging from simple single-celled organisms (cyanobacteria and bacteria) to complex mammals, have biological rhythms [7,8]. Circadian rhythm refers to the regular behaviours exhibited through the behavioral characteristics of animals to adapt to circadian changes. The peak of activity of diurnal animals mainly occurs during the daytime when it is light, and their body temperature and hormone levels reach the highest level during the day, while at night, the majority of their activities and physiological indexes decrease. In contrast, the activities and physiological indexes of nocturnal animals show the opposite trend [9]. The critical regulatory center of these activities is the circadian clock, which includes a central clock and peripheral clock. The circadian clock allows for the transient regulation of an organism by controlling the expression of circadian rhythm genes and behavioral activity. The origin and complexity of circadian clocks in different circadian rhythms may be different, but at the core there is always an internally spontaneous rhythm oscillator. There are positive and negative regulatory elements in the spontaneous rhythm oscillator, forming an auto-regulatory feedback loop, completing an approximately 24 h rhythm cycle [10,11], regulating the physiological and behavioral rhythms of the body.

The abalone *Haliotis discus hannai* is an economically important marine shellfish species in China. The aquaculture production of this species was 163,300 tons in 2018, accounting for over 90% of the world's total yield [12]. In the natural environment, abalone inhabits

* Corresponding authors at: College of Ocean and Earth Sciences, Xiamen University, 116023 Xiamen, Fujian Province, China.
E-mail addresses: wwyou@xmu.edu.cn (W. You), chke@xmu.edu.cn (C. Ke).

https://doi.org/10.1016/j.jphotobiol.2020.111994
Received 7 April 2020; Received in revised form 21 July 2020; Accepted 9 August 2020
Available online 12 August 2020
1011-1344/

rocky reefs that are characterized by a diversity of seaweeds and unobstructed water flow. This species is unlikely to gather in masses when exposed to sunlight, but is more often found on the lee side and in shade. As a typical nocturnal creature, abalone often takes in food and moves at night, while evading light by hiding in the shade during the day [13]. Under artificial indoor culture conditions, feeding often takes place in the evening, and a conventional practice for the optimization of the light environment is to put up a black sunshade net and lay square bricks as a means of evasion. García-Esquivel et al. [14] reported that *Haliotis fulgens* showed the highest growth rate under a constant dark regime. In the dark, the survival rate and food intake rate of *Haliotis corrugata* larvae was significantly higher than those in constant light [15]. In light conditions, the oxygen consumption rate and ammonia excretion rate of *H. discus discus* was significantly higher than those of the group in the dark [16]. In a lightproof water tank, the growth rate of *Haliotis rubra* was 15.65% faster than that in light conditions [17]. *H. discus hannai* has an obvious tendency to select a dark environment and red and orange light with long wavelengths, but to evade green, blue, and purple light with short wavelengths [18]. In 0 L:24D, 4 L:20D, and 8 L:16D, the cellulase and pepsin activities of *H. discus hannai* were significantly higher than those in 12 L:12D and 16 L:8D [19]. The majority of current research on the behavioral rhythms of abalone are subject to experience-based judgment and there is an urgent need for a detailed quantitative description. However, the potential physiological mechanisms that produce differences in circadian rhythms have not yet been reported. Provided with a sufficient food supply, there is a lack of basic data supporting whether the behaviour and circadian rhythms of abalone are a form of passive selection for the purpose of evading enemies and improving food availability or an active adaptation to the changes in light cycle subject to the regulation of the biological clock.

In this research, a quantitative study was carried out to determine the movement behaviours of abalone using time-lapse photography technology at the individual level. The key indexes of movement were quantified using professional behaviour analysis software, in order to reveal the variations in the circadian movement behaviours of abalone. The physiological and metabolic differences of abalone were identified by ultra-performance liquid chromatography and mass spectrometry (LC-MS). The results of this study will enrich the basic knowledge abalone behaviour and ecology and provide scientific references for optimizing the light environment and feeding strategy during aquaculture production.

2. Materials and Methods

2.1. Experimental Abalone

Juvenile abalone (shell length 9.89 ± 0.57 cm, body weight 92.17 ± 1.83 g) were purchased from Fuda Abalone Aquafarm (Jinjiang, Fujian), and all experimental abalone were sourced from the same stock after artificial hatching. Prior to the experiment, 30 abalone were placed in two culture tanks (0.8 m long × 0.4 m wide × 0.4 m high) with a 12 L:12D light cycle to acclimatize for 15 days. Light-emitting diodes were provided by the Shenzhen Fluence Technology PLC (Guangdong, China), the white-light lamp (5 W, $\lambda_{400-780\ nm}$) was full spectrum to simulate natural light. The seawater was changed once a day, and continuous aeration was provided. Water temperature was maintained at 19 °C, the salinity was 30 ± 1, pH was 8.2, and the concentration of dissolved oxygen was > 6 mg/L. The water used in the culture system was sourced from the natural sea area and was subject to sedimentation and sand filtration prior to use. The abalone were fed with fresh *Gracilaria lemaneiformis* every day, equivalent to 5% of the wet body weight of abalone, in order to ensure they reached a state of satiation.

2.2. Experimental Units

The behaviour monitoring device was comprised of two components: a breeding experiment unit and video surveillance unit. The round polyethelene tank was 1.2 m in diameter and 0.35 m high. The experimental tank was covered with a shade cloth to completely block external light. LEDs were used as built-in light sources during the experimental period. The movement behaviour of abalone was recorded with an infrared camera (HIKVISION, Hangzhou, China), located above the center of the experimental tank. The vision field of the camera reached the outer bottom edge of the experimental tank and the light intensity at the bottom of the experimental tank was approximately 31.04 ± 9.73 lx. Experimental videos were collected and stored using the video surveillance unit and the light cycle (12 L:12D) was controlled with a clock controller. The total recording time was 24 h, with a 5 s time interval. The video was in AVI format with a video resolution of 680 × 480 pixels and 10 frames per s.

2.3. Experimental Design

After the acclimatization period, the abalone were placed in the experimental tank for 2 h to adapt to the experimental conditions. A single abalone was selected for each experiment, which lasted 24 h, with a 12 L:12D light cycle. Light was turned on and off at 06:00 h and 18:00 h, respectively. During the experimental period, no feeding or water exchange was carried out. One abalone was replaced before each experiment, with a total of 30 experimental abalone. After the experiment, the abalone was placed into another culture tank and was not reused during the behaviour experiment. The videos recording behaviour were analyzed using XT Ethovison 9.0 behaviour analysis software (Noldus Information Technology, Wageningen, Netherlands). The measurement indexes used include movement distance, accumulated movement time, average movement speed and maximum movement speed of each abalone.

When the movement behaviour experiment was completed, each abalone acclimatized under the above-given light cycles was wiped with a sterile gauze until the body surface was dry. Cerebral ganglion sample was extracted at 06:00 h (6 M), 14:00 h (14 M), and 22:00 h (22 M). The samples were placed in a 1.5-mL centrifuge tube and immediately transferred to liquid nitrogen for metabolomic assessment. A total of six abalone were sampled at each of the time points.

2.4. Extraction of Metabolites

A 30-mg sample, was added to 20 μL of each of the internal standard substances (L-2-chlorophenylalanine, 0.3 mg/mL; Lysophosphatidylcholines (lysoPC) 17:0, 0.01 mg/mL, prepared by methanol). This was then added to a 400 μL methanol solution (V_{CH3OH}: V_{H2O} = 4:1). Two small steel balls were added and the solution was kept at −20 °C for 2 min, before being transferred to a grinder (60 Hz, 2 min). Extraction was then carried out ultrasonically in a water bath for 10 min. The sample was then allowed to settle at −20 °C for 20 min. After being centrifuged for 10 min (13,000 rpm, 4 °C), 200 μL of supernatant was extracted with a syringe, filtered with a 0.22-μm organic phase syringe filter, transferred to a LC vial and stored at −80 °C until LC-MS was conducted. Quality control (QC) samples were prepared with the extracts of all samples and the volume of each QC sample was the same as the experimental sample.

LC-MS was carried out using an ACQUITY UPLC Ultra High Performance Liquid Chromatograph (Waters, Milford, Massachusetts, USA) in serial connection with an AB Triple TOF 5600 High Resolution Mass Spectrometer (AB Sciex, Redwood, CA, USA). An ACQUITY UPLC BEH C-18 chromatography column (100 mm × 2.1 mm, 1.7 μm). The column temperature was 45 °C and the mobile phase comprised A-water (with 0.1% formic acid), and B-acetonitrile (with 0.1% formic acid). The flow rate was 0.4 mL/min and the injection volume was 5 μL. The

ion source was ESI and sample MS signal was acquired using the positive and negative ion scanning mode.

2.5. Data Preprocessing

Data were preprocessed prior to pattern recognition. The raw data went through baseline filtering, peak identification, integration, retention time correction, peak alignment, and normalization using metabolomics processing software, Progenesis QI v2.3 (Nonlinear Dynamics, Newcastle, UK). The main parameters were a precursor tolerance of 5 ppm, a product tolerance of 10 ppm, and a product ion threshold of 5%. Compounds were identified based on exact mass number, secondary fragments and isotopic distribution, and were qualified using the Human Metabolome Database (HMDB), Lipidmaps (v2.3) and the METLIN database. For extracted data, the ion peaks with missing values (0 values) > 50% in groups were deleted, the qualified compounds were screened according to the qualitative result scores of compounds. The screening standard was 30 points (full score: 60 points) and any compound with a score of 30 or less was considered to have inaccurate qualitative results and thus, deleted.

2.6. Data Analysis

All data were statistically analyzed by SPSS 18.0. Prior to data analysis, the normal distribution and homogeneity of variance of all data were validated by Kolmogorov-Smirnov and Levene's test. The differences in the movement behaviour indexes of the abalone were examined by one-way analysis of variance and Tukey's multiple comparisons. All data were presented as mean ± standard error (mean ± SE) and P values < 0.05 were statistically significant. The data obtained from this analysis were plotted on SigmaPlot.

The cosine fitting of behavioral data was performed using the Cosinor package in Matlab software, $Y = M + A\cos(\omega t + \Phi)$ functioning as the calculation model. M (MESO) represents the median value of the fitted cosine curve, A, ω, and Φ represent the amplitude, angular frequency, and peak value of the cosine fitting respectively. The t represents the circadian time over 24 h, Y represents the movement behaviour parameters of abalone at each time point measured at an interval of 3 h. Finally, the respective values of M, A and Φ in the cosine fitting curve were calculated [20].

The data matrix was imported into the SIMCA software package (version 14.0, Umetrics, Umeå, Sweden), the overall distribution between samples and the stability throughout the analysis process were observed through unsupervised principal component analysis (PCA), then the overall differences in metabolic profiles between groups were differentiated through Orthogonal Projections to Latent Structures Discriminant Analysis (OPLS-DA) to identify the differential metabolites between groups. Differential metabolites between groups were screened using multidimensional analysis in combination with unidimensional analysis. In the process of OPLS-DA, variable importance in projection (VIP) was used to measure the influence and explanatory power of the expression pattern of each metabolite on the classification and discrimination of each group, and metabolites with VIP > 1 were considered as differential metabolites. Furthermore, the *t*-test (Student's *t*-test) was used to verify whether differential metabolites between groups were significant or not. The screening criteria for the first principal component of the OPLS-DA model was VIP > 1, $P < 0.05$. The enrichment analysis of metabolic pathways was performed based on the KEGG database (http://www.genome.jp/KEGG/pathway.htmL). Differential metabolites were mapped to the KEGG database in order to obtain the enrichment results of metabolic pathways, $P < 0.05$ was considered as significant enrichment.

Table 1
The cosine rhythm characteristics of behavioral parameters in *Haliotis discus hannai*.

Behavioral parameters	Mesor (M)	Amplitude (A)	Acrophase (φ, hh:mm)	*P*-value
Distance moved	4730.73	6954.74	00:46	0.011
Cumulative duration of moving	2790.83	2877.52	00:38	0.012
Maximum velocity	3.151	0.392	02:59	0.011
Mean velocity				0.477

3. Results

3.1. Movement Behaviour Analysis of Abalone over 24 H

After continuous observation for 24 h, the cumulative movement distance of abalone was 37,843 ± 2451 mm, while the continuous movement time was 22,324 ± 1967 s. The average movement speed was 1.7 ± 0.18 mm/s, and the maximum movement speed was 3.15 ± 0.40 mm/s.

The results from the cosine analysis showed that the cumulative movement distance of abalone over 24 h showed significant diurnal cosine rhythms (Table 1, $P < 0.05$). The cumulative movement distance of abalone from 00:00–03:00 h was significantly higher than any other time period (Fig. 1a, $P < 0.05$). The cumulative movement distance of abalone from 21:00–00:00 h and 03:00–06:00 h was less than that from 00:00–03:00 h, but each was significantly more than that in the other time periods ($P < 0.05$). The cumulative movement time of abalone over 24 h show significant diurnal cosine rhythm (Table 1, $P > 0.05$). A significant difference was identified in respect of the cumulative movement time of abalone between 00:00–03:00 h and 03:00–06:00 h, but each was significantly longer than that in any other period (Fig. 1b, $P < 0.05$). The cumulative movement time of abalone from 06:00–09:00 h was significantly shorter than that between 15:00–18:00 h, but it was significantly longer than that in the 09:00–12:00 h and 12:00–15:00 h time periods ($P < 0.05$).

The maximum movement speed of abalone showed significant circadian rhythms, but average movement speed of abalone did not show any significant diurnal cosine rhythm (Table 1, $P > 0.05$). From 09:00–12:00 h, 12:00–15:00 h, 03:00–06:00 h, and 06:00–09:00 h, no significant difference was identified in respect of the maximum movement speed of abalone, but each was significantly higher than that between 21:00–00:00 h (Fig. 1c, $P < 0.05$). The minimum value of the average movement speed of abalone occurred between 12:00–15:00 h, its average movement speed during this time period was not significantly different from that in between 09:00–12:00 h, 21:00–00:00 h, and 06:00–09:00 h, but it was significantly lower than the other time periods (Fig. 1d, $P < 0.05$).

3.2. Base Peak Chromatogram

BPC (Base Peak Chromatogram) is a graph obtained by continuously plotting the ions with the highest intensity in the mass spectrum at each time point. Through the extraction and detection of abalone metabolites in 6 M, 14 M, and 22 M, the positive ion BPC graph in the control sample (prepared by mixing the extracts from all samples in equal volume) contained 14,394 substance peaks and 3516 metabolites were screened and obtained. The negative ion BPC graph contained 12,141 substance peaks and 2077 metabolites were screened and obtained (Fig. 2).

3.3. PCA Analysis of all Samples

The PCA model graphs for *H. discus hannai* samples at each sampling time were obtained through 7-fold cross-validation (Fig. 3). Through

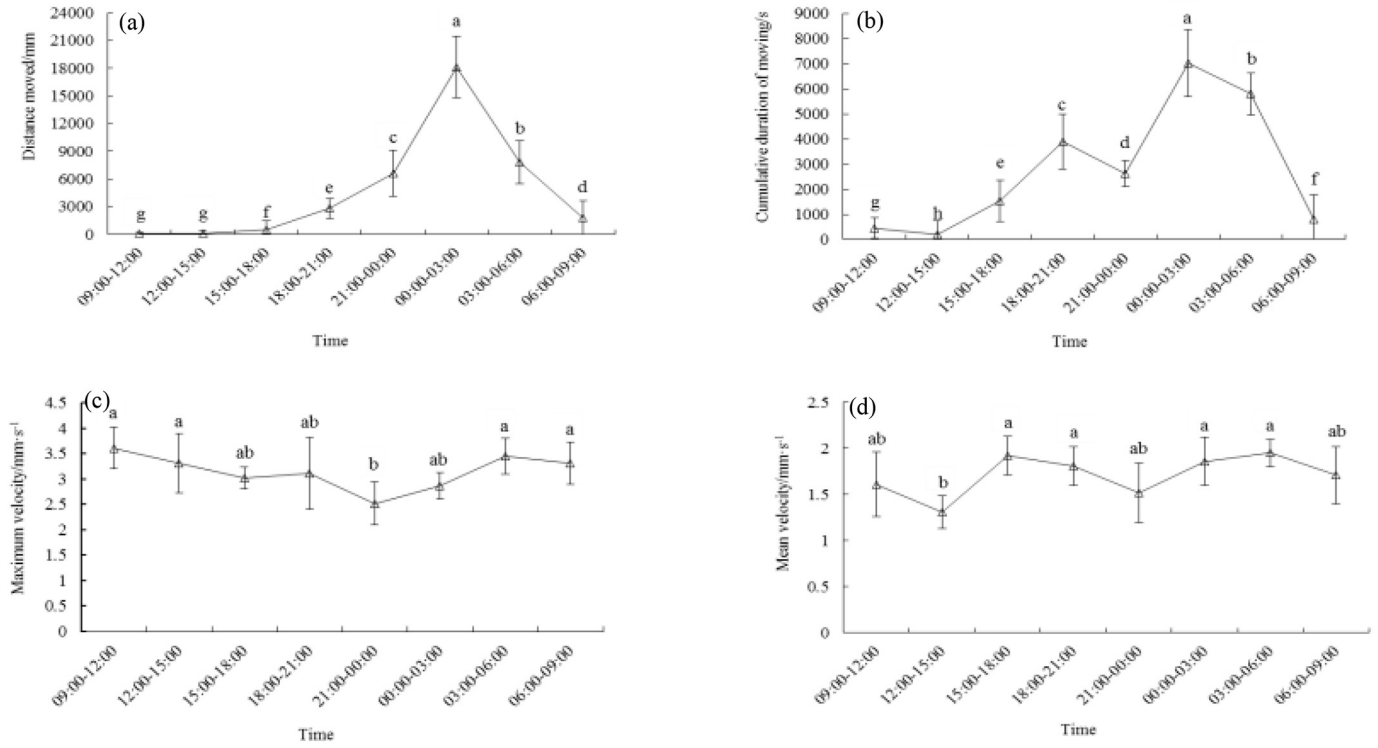

Fig. 1. Locomotory performance of *Haliotis discus hannai* at 12 light:12 dark: (a) distance moved; (b) cumulative duration of moving; (c) maximum velocity and (d) mean velocity. Data are means and standard deviations, sample size = 30. Significant variations were found by one-way analysis of variance, $P < 0.05$, followed by Tukey test. Different letters denote significant differences between time periods.

the PCA analysis, it was found that all samples were within the 95% confidence interval of Hotelling's T2 test, suggesting that PCA dimension reduction can better predict and explain these samples. QC samples were tightly clustered, indicating that the stability and repeatability of this experiment was good.

3.4. Multivariate Statistical Analysis of Two Sample Sets and RPT of OPLS-DA Model

By comparing the scatter plots and permutation test patterns for OPLS-DA scores between every two samples of the three sampling times, it was found that two treatment samples differentiated significantly in the predicted score for the first principal component (t [1]), both samples were within the 95% confidence interval (Hotelling's T2), and samples with different sampling times were clearly differentiated based on OPLS-DA analysis (Fig. 4). In order to prevent the proposed model from overfitting, 200 response permutation tests (RPT) were conducted on the OPLS-DA model. To be more specific, the X matrix was fixed, the predefined variables (like 0 or 1) of the classification Y matrix were randomly permutated n times ($n = 200$) and the corresponding OPLS-DA model was established to obtain the R2 and Q2 value for the random model. Linear regression was performed with R2Y and Q2Y of the original model and the regression line and the y-axis were R2 and Q2, respectively. The predictability of the proposed model for the differential metabolism between 22 M and 14 M, 6 M [R2(Y)] was 96.00% ~ 99.30%, the cross-validity verification showed that the average predictability Q2Y was 52.20% ~ 80.50, and Q2Y was greater than 50%, indicating that this model had a good predictability. The permutation verification results from the OPLS-DA analysis derived that the regression line intercept, which was composed of the R2Y (as shown in the green circle) and the R2Y of the real model was 0.915–0.987, and that the regression line intercept which was composed of Q2Y (as shown in the blue diamond) after 200 modeling trials, and the Q2Y of the real model was −0.507 ~ −0.162. The above results showed that the established pattern recognition model was effective with no occurrence of overfitting.

3.5. Identification and Analysis of Differential Metabolites

The 380, 385, and 315 metabolites with significant differences were identified from 6 M vs 14 M, 14 M vs 22 M, and 6 M vs 22 M, respectively. Most differential metabolites were identified from 14 M vs 22 M, including prenol lipids (phytocassane C, cyrneine A, phytocassane B, etc.), organic oxygen compounds (voglibose, *N*-acetylneuraminic acid, *N*-acetylgalactosamine, et al.), fatty acyls (ent-11-epi-8-E2t-IsoP, 12-HEPE, 1a,1b-dihomo-PGD2), and organoheterocyclic compounds (hypoxanthine). The differential metabolites identified from 6 M vs 14 M also included glycerophospholipid (lysoPC(20:5(5Z,8Z,11Z,14Z,17Z)), lysoPC(16:1(9Z)/0:0), lysoPC(22:4(7Z,10Z,13Z,16Z)), etc.), fatty acyls (9,10,18-TriHOME(12), 9,12-dihydroxy stearic acid, N-(5-hydroxy-pentyl) arachidonoyl amine), pyrimidine nucleotides (dTDP-4-acetamido-4,6-dideoxy-D-galactose, dTMP, etc.), purine nucleosides (xanthosine, deoxyinosine, inosine, guanosine 3′-diphosphate 5′-triphosphate), and organoheterocyclic compounds (serotonin). The differential metabolites identified from 6 M vs 22 M also include fatty acyls (prostaglandin D1, ent-11-epi-8-E2t-IsoP, 8-deoxy-J2-IsoP), prenol lipids (phytocassane C, (−)-enuniceline, cyrneine A, etc.), steroids and steroid derivatives (pregnanetriol, 15 beta-Hydroxydesogestrel) (Supplementary Table 1). To show the relationship between samples and the differential expression of metabolites between different samples more intuitively, hierarchical clustering was performed on the expression levels of the Top50 metabolites with significant differences, and the expression levels of differential metabolites were visualized based on VIP values (Fig. 5).

3.6. KEGG Annotation of Differential Metabolites

Pathway enrichment analysis was conducted using the KEGG ID of

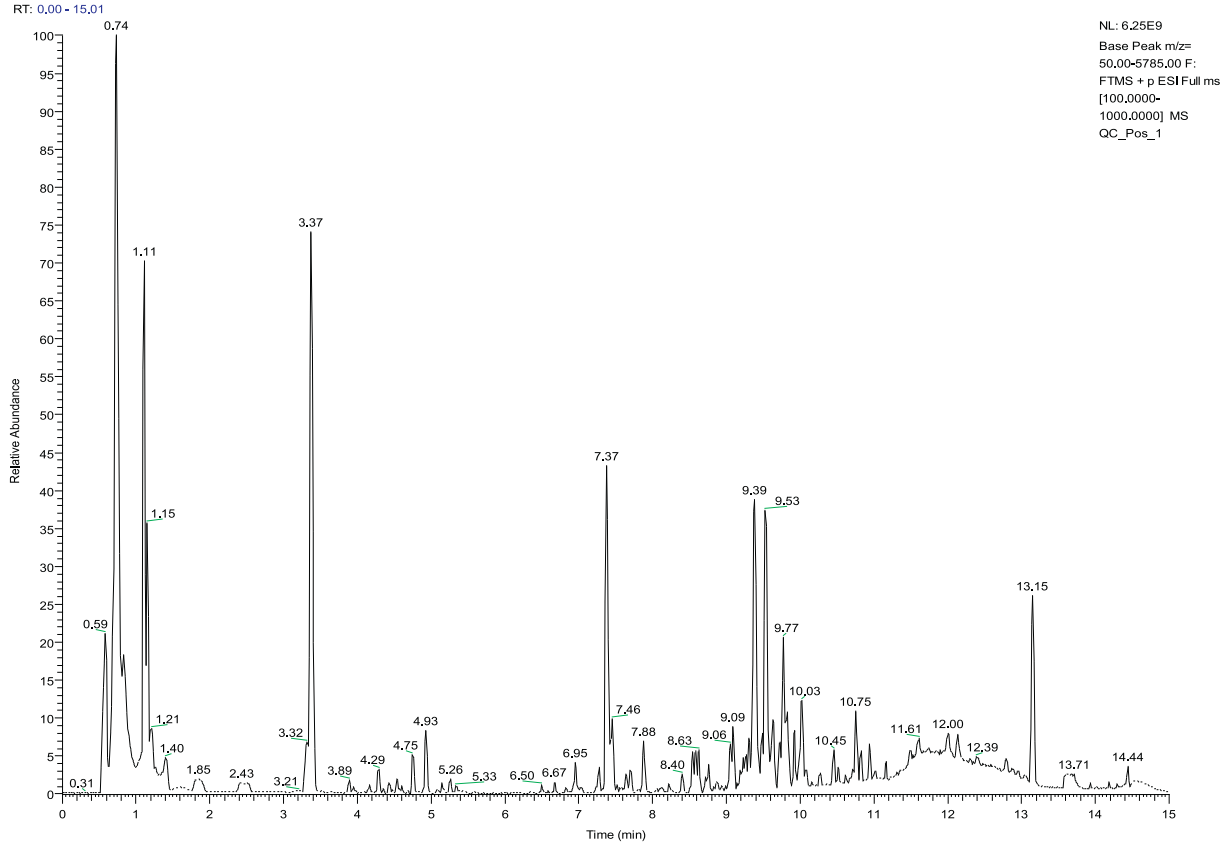

(a)

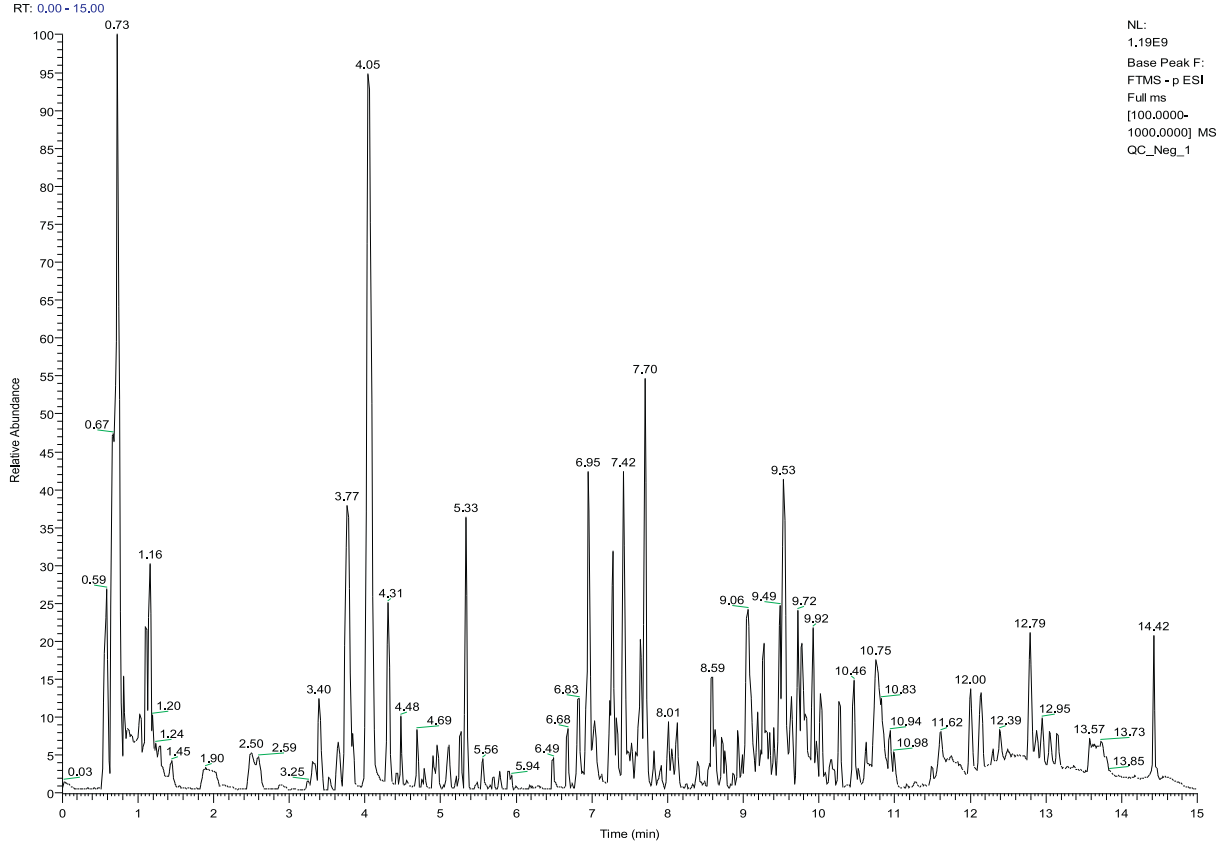

(b)

Fig. 2. The base peak chromatogram of positive (a) and negative (b) ion of quality control samples by liquid chromatography mass spectrometry (LC-MS).

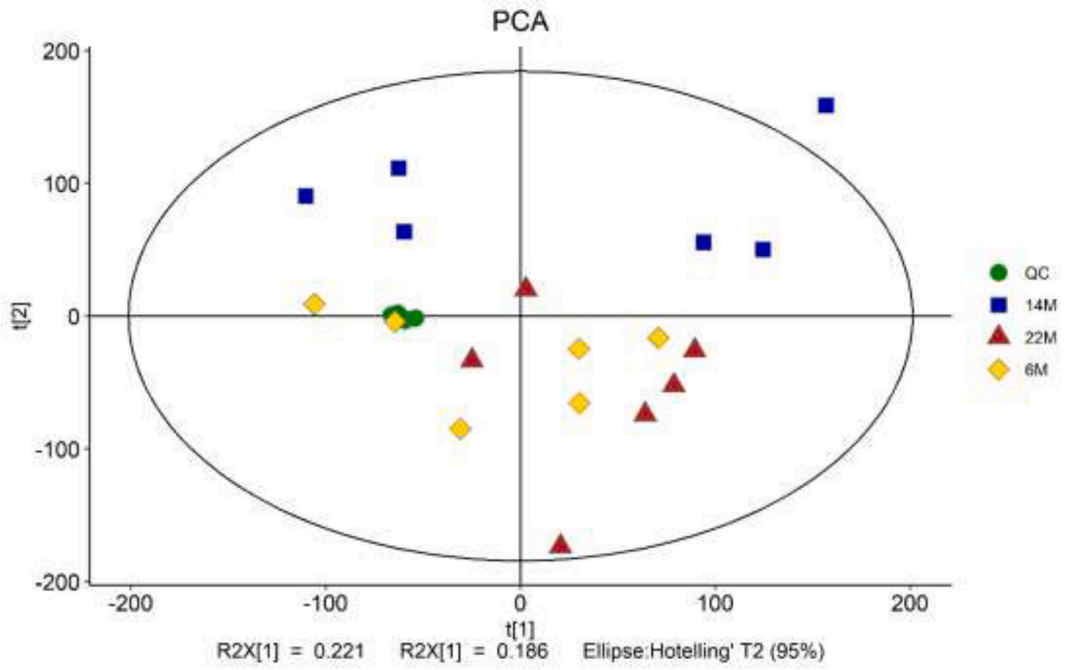

Fig. 3. Score scatter plot of the principal component analysis (PCA) model for metabolites in the cerebral ganglion of *Haliotis discus hannai* at different sampling times (06:00, 6 M; 14:00, 14 M; 22:00, 22 M).

differential metabolites to obtain the results of metabolic pathway enrichment. In 6 M vs 14 M, 14 M vs 22 M, and 6 M vs 22 M, 33, 44, and 30 metabolic pathways were enriched respectively, of which eight, 10, and seven were significantly enriched. In particular, the arachidonic acid metabolism pathway was significantly enriched in each comparison group ($P < 0.05$), while linoleic acid metabolism was significantly enriched in 6 M vs 14 M and 6 M vs 22 M ($P < 0.05$). Purine metabolism, tryptophan metabolism, and glycerophospholipid metabolism were significantly enriched in 14 M vs 22 M and 6 M vs 14 M ($P < 0.05$, Fig. 6).

4. Discussion

Movement behaviour is an integral part of all animal behaviours and is essential for the normal functioning of predatory behaviour, anti-predatory behaviour and migration behaviour. In this sense, the ability to move can be crucial for the survival of an animal [21–23]. Although there are vast differences in the movement behaviours of abalone during the day and night, there is no adequate quantitative description of these behaviours. The information available comes largely from visual observations and empirical judgment and there is no reference for light control and selection of feeding time and frequency during aquaculture production. In this research, analysis of video recordings revealed that the cumulative movement distance of abalone was the highest between 00:00–03:00 h, followed by that 21:00–00:00 h and 03:00–06:00 h. This result coincides with the nocturnal behaviour rhythms of abalone. Two peak values of cumulative movement time of abalone were recorded, with the maximum value also occurring from 00:00–03:00 h, and the other peak occurring from 18:00–21:00 h. This indicated that abalone could clearly sensed the changes in the external light environment, such as the onset of darkness once the lights were switched off. The changes in the light environment may serve as a factor inducing the alteration of the metabolic function in abalone. The accumulative movement distance from 18:00–21:00 h was less than that from 00:00–03:00 h, but a significant increase in cumulative movement time compared to previous points might also be an active adaptation to environmental changes. Gao et al. [18] also found that the response time and the time required for overturning and standing of *H. discus hannai* under blue and green light with a short wavelength were significantly shorter than that under red light, orange light and dark environment. This reaffirms that abalone can quickly perceive changes in external light environment factors, and actively drive the body to make adaptive changes.

The lowest average movement speed occurred between 12:00–15:00 h, during which time the average movement speed of abalone was low and the corresponding cumulative movement time was the shortest subject to the light impact. However, the highest value of the maximum movement speed occurred between 09:00–12:00 h, during which time period the cumulative movement distance and cumulative movement time were shorter. Fast movements are likely to be an active evasion to avoid light. Extensive observations in natural seas have shown that *Haliotis laevigata* seldom moves in areas with sufficient inshore reef cracks, but tend to have a drastic increase in movement frequency with a decrease in the available crack spaces [24]. Sea urchins generally hide in the cracks of rock reefs during day, but crawl out at night to feed [25,26]. Field observations show that *Haliotis midae* are often hidden under *Parechinus angulosus* during the day, and even at night, only 10–25% of *H. midae* choose to leave *P. angulosus* to take in food. *H. midae* that are hidden under *P. angulosus* will drastically improve their ability to acquire food with reduced energy output [27]. The activity rhythms of *Apostichopus japonicas* also show obvious circadian patterns. Dong et al. [28] found that *A. japonicas* was active under low light intensity, and the exposure index would increase significantly with the extended length of dark time. Mercier et al. [29] reported that small *Holothuria scabra* only feed at night to evade predators. Following metamorphosis, *Cucumaria frondosa* also hides in the shade of rock cracks until it has reached adulthood, similar to *H. scabra* [30]. The results of the current study show that abalone has obvious circadian rhythms and movement behaviours that may change with the external light environment, which are likely associated with the internal biological clock mechanism developed from long-term evolution. For slow-moving organisms that solely rely on the forced protection of shells, such as abalone, it is considered “wise” to stagger movement behaviours to the feeding peak of predators, to evade threats from harmful organisms.

Metabolomics is an important tool applicable to systems biology,

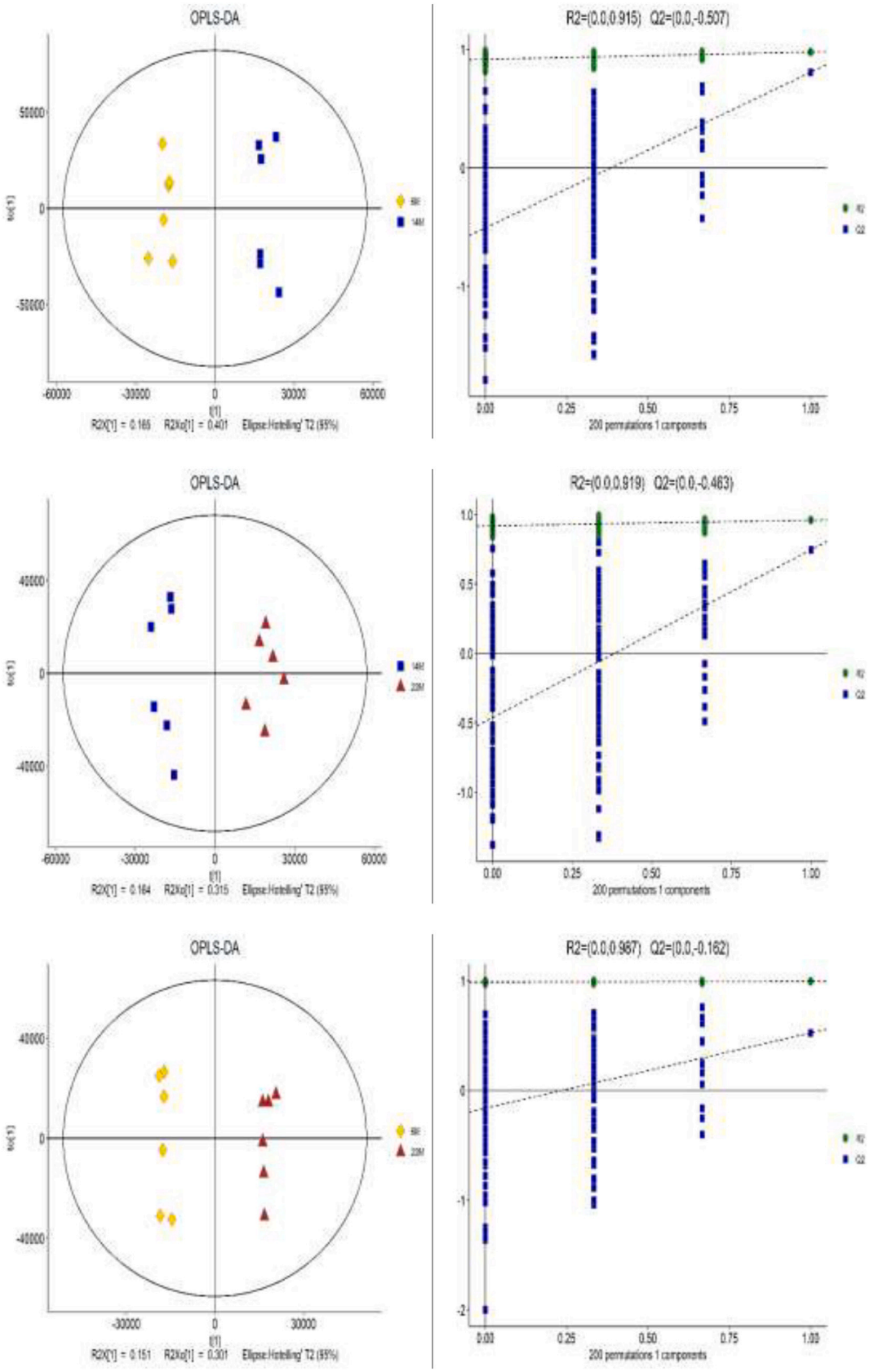

Fig. 4. Score scatter plot and permutation test of OPLS-DA model for metabolites in the cerebral ganglion of *Haliotis discus hannai* in 6 M vs 14 M, 14 M vs 22 M and 6 M vs 22 M.

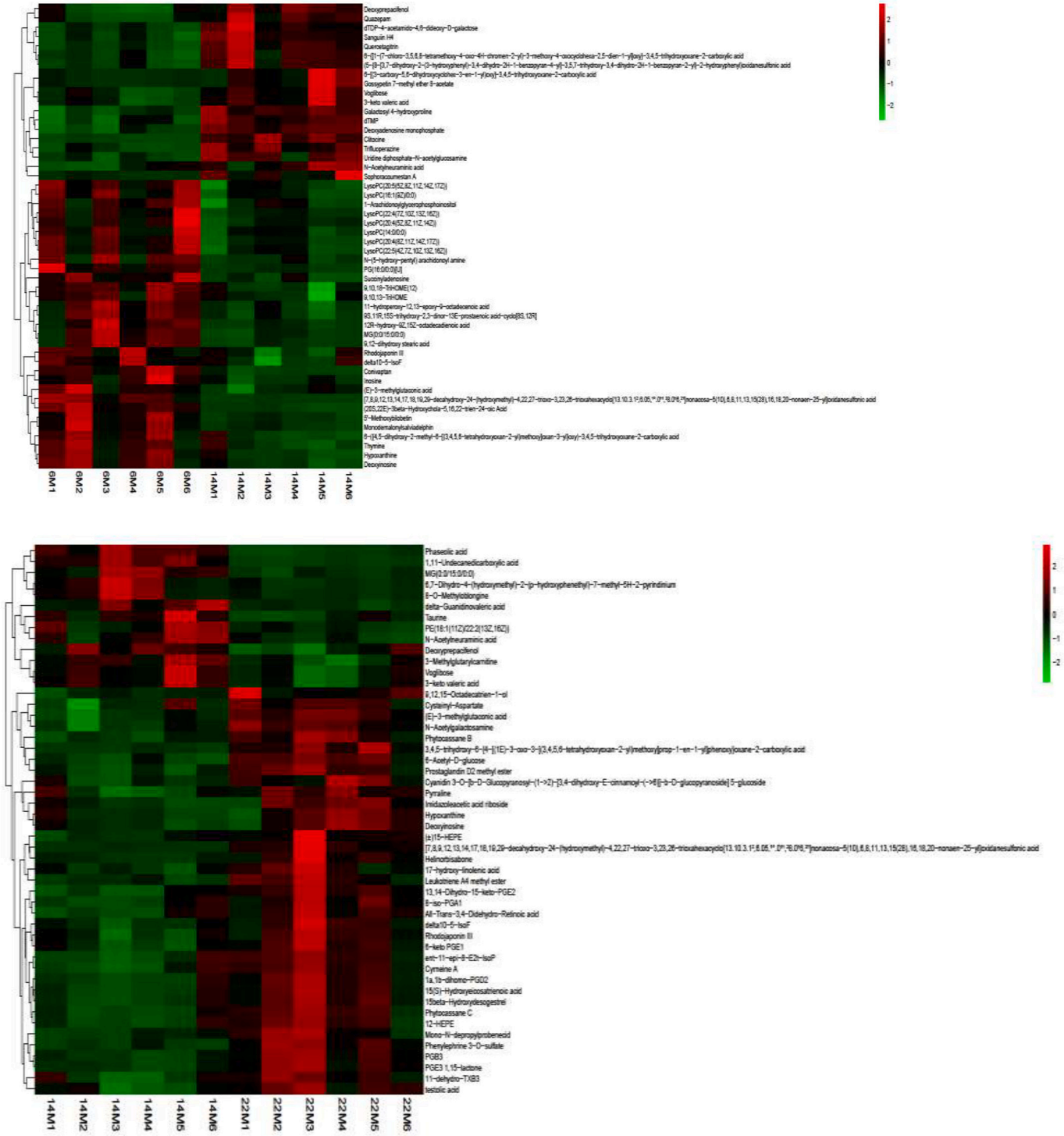

Fig. 5. Hierarchical clustering analysis for the top fifty significantly different metabolites in 6 M vs 14 M, 14 M vs 22 M and 6 M vs 22 M. The relative metabolite level is depicted according to the color scale. Red indicates upregulation, and green indicates downregulation. (For interpretation of the references to color in this figure legend, the reader is referred to the web version of this article.)

which can measure the concentration of endogenous small molecules in biological fluids, and determine changes in the number of metabolites generated under particular physiological states of a living organism [31]. Arachidonic acid is a polyunsaturated ω-6 fatty acid, which can serve as a precursor to many bioactive lipid mediators and play an underlying role in muscle anabolism [32]. In this study, the arachidonic acid metabolism pathway was significantly enriched in each group, and the expression levels of phosphatidylcholine in this pathway were significantly upregulated in 6 M vs 14 M, but those in 14 M vs 22 M were significantly downregulated, indicating that the expression levels of phosphatidylcholine would reduce in dark periods, but rise in light conditions. Arachidonic acid is catalyzed by the cytochrome P450 enzyme in the body to generate epoxyeicosatrienoic acids, reactive oxygen species and 20-hyeroxyeicosatetraenoic acids [33]. Epoxyeicosatrienoic acids can open up ATP-sensitive potassium channels (KATP) to place smooth muscle cells in a hyperpolarized state, relax

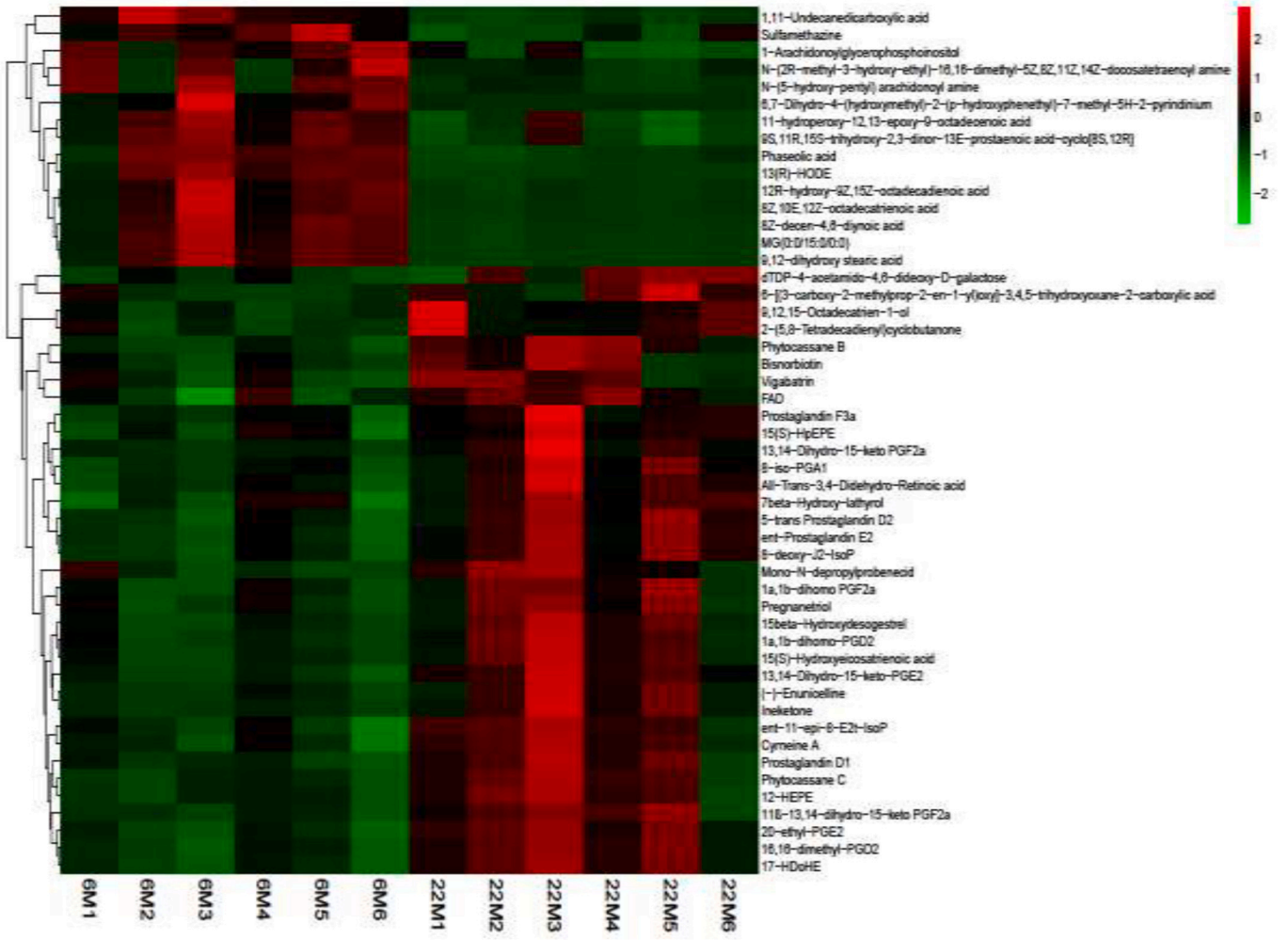

Fig. 5. (*continued*)

blood vessels, and participate in blood pressure regulation. It can also inhibit the migration of smooth muscle cells by activating the cAMP-PKA signaling pathway, and promote the release of peptide hormones and cell proliferation and migration [34,35]. It is well-known that K^+ ion channels are closely related to cell signaling. Arachidonic acids can also inhibit the activity of myosin phosphatase, leading to an increased sensitivity of smooth muscle to calcium ions, and the release of Ca^{2+} can activate the contraction of smooth muscle [36]. In this sense, once the arachidonic acid metabolism pathway is activated, the K^+ ion channels in muscle cells can in turn be activated, thereby affecting the signaling of muscle cells, and facilitating the enhanced sensitivity of these muscle cells to Ca^{2+}. As a result, the muscle contractility will be influenced, which is probably an underlying physiological mechanism that causes significant differences in the nocturnal movement behaviour of abalone.

Phospholipids are the skeleton components of cell membranes and organelle membranes in animals and plants, its bi-layer structure can maintain the transfer of material and information in and out of the membrane. Once activated, the membrane receptor will lead to the decomposition of specific phospholipid components on the membrane and generate an intracellular second messenger, thus regulating cell growth and metabolism. As a result, cell growth and metabolism can be regulated by modifying the content of membrane phospholipids and the composition of fatty acids [37,38]. In 14 M vs 22 M and 6 M vs 14 M, the Glycerophospholipid metabolism pathway was significantly enriched, with the expression levels of LysoPC (20: 5 (5Z, 8Z, 11Z, 14Z, 17Z)), LysoPC (22: 4 (7Z, 10Z), 13Z, 16Z)) and phosphatidylethanolamine (PE) (18: 1 (11Z) / 22: 2 (13Z, 16Z)) significantly increasing, indicating that these metabolites have engaged in the conversion of abalone physiological adaptation mechanism at day and night. It was reported that phospholipid composition is crucial to certain functions related to mitochondria, cell growth, muscle contraction, movement performance, and sensitivity of insulin in skeletal muscles [39]. When the enzymes associated with the synthesis of phosphatidylcholine (PC) and PE were knocked out, mice were subject to reduced synthesis of PE and an increased PC:PE ratio. Not only did the skeletal muscle reduce, the Ca^{2+} ATP enzyme activity on endoplasmic reticulum/sarcoplasmic reticulum and the movement ability reduced [40,41]. Therefore, when the content of PE and PC changes between day and night, the fluidity and permeability of cell membranes are also likely to change, thus affecting cell physiology and function. This transition process plays a crucial role in regulating the plasticity of animal behaviours [42]. In the above two treatments, an increase in the expression levels of PE and PC also coincided with the lighting periods, during which the cumulative movement distance and cumulative movement time of abalone were shorter, but the maximum movement speed and average movement speed were faster. It can therefore be inferred that PE and PC participated in the process of underlying physiological regulation that involves muscle contraction, enhanced movement ability and movement efficiency of abalone.

Tryptophan is a class of amino acid with metabolic activity, 5-hydroxytryptamine (5-HT) and kynurenine serve as two metabolic pathways. The neurotransmitter 5-HT is a metabolite of tryptophan which can neutralize adrenaline and norepinephrine, thereby inhibiting the

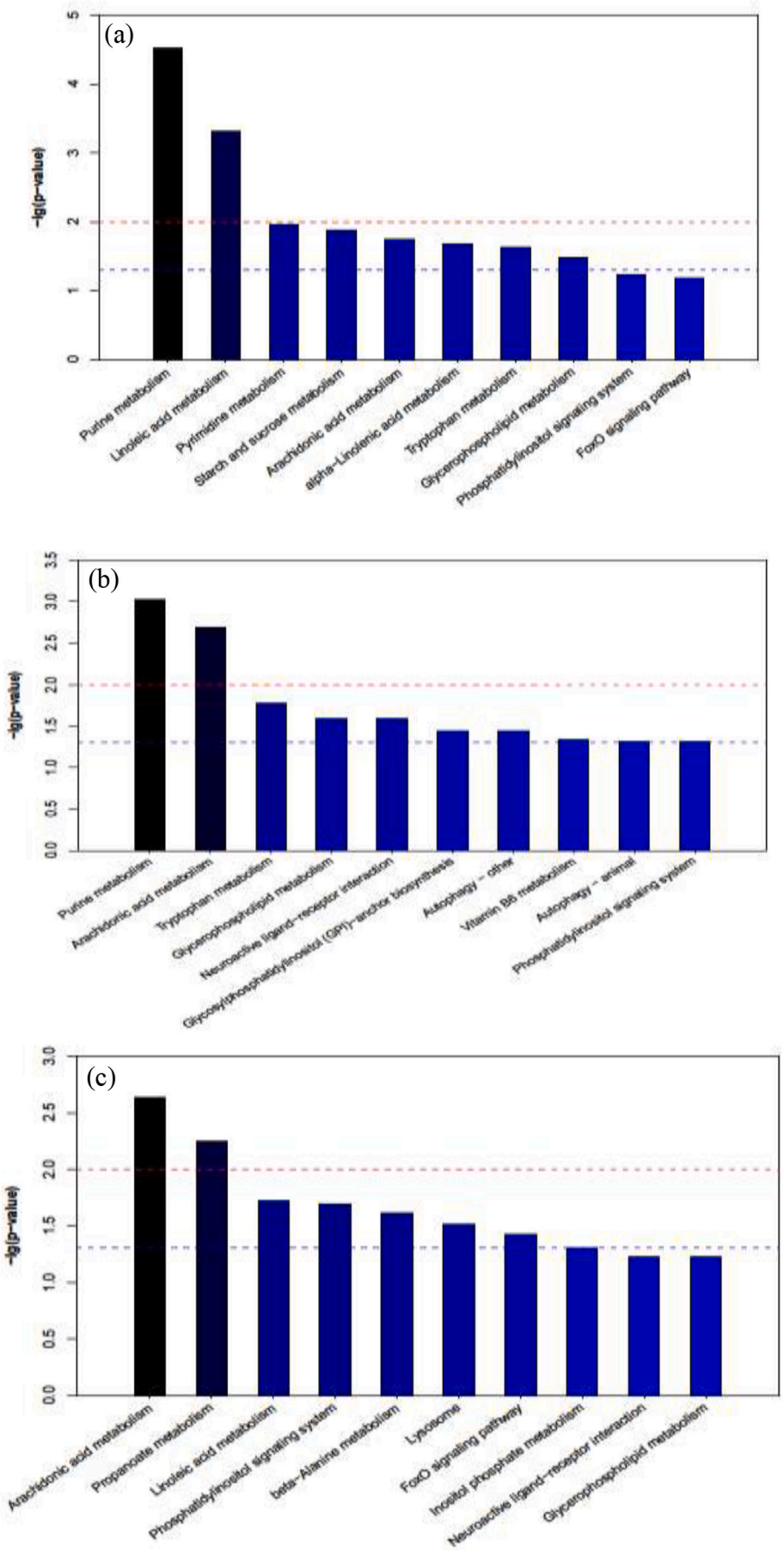

(caption on next page)

Fig. 6. Metabolic pathway enrichment analysis in the 6 M vs 14 M (a), 14 M vs 22 M (b), and 6 M vs 22 M (c) treatments. The x-axis represents pathway enrichment, and the y-axis represents the pathway impact. The blue dashed line indicates $P < 0.05$, the red dashed line indicates $P < 0.01$. The darker the bar color, the more significant the difference in metabolic pathways. (For interpretation of the references to color in this figure legend, the reader is referred to the web version of this article.)

transmission of neurotransmitter impulses and improving the anti-stress and immune regulation capacity [43]. In 6 M vs 14 M and 14 M vs 22 M, the tryptophan metabolism pathway was significantly enriched. Among that, the metabolites 5-HT, *N*-acetyl-5-hydroxytryptamine, and indole-3-acetaldehyde were significantly upregulated in 6 M vs 14 M, indicating that the light environment may stress abalone. The increased concentration of 5-HT enhances the environmental adaptation of an organism. Melatonin extensively participates in the regulation of life processes such as circadian rhythms, neuroendocrine, and growth and development [44]. 5-HT, the synthetic precursor of melatonin, can generate N-Acetyl-5-hydroxytryptamine under the action of Aralkyl amine *N*-acetyl transferase, indicating that the synthesis of melatonin increases during light periods, but its synthesis secretion reduces at night. This result is in contrast with the secretion of melatonin from a diurnal organism, which peaks at night and degrades under light conditions during day. However, the results are consistent with the diurnal habits of abalone. Melatonin, 5-HT and *N*-acetyl-5-hydroxytryptamine, the metabolites of tryptophan, can function as scavenging free radicals, inhibiting the production of superoxide compounds, facilitating the proliferation and differentiation of T and B cells, and enhancing the sensitivity of antibodies to antigens [45,46]. This also indicates that an increased concentration of 5-HT, for example, is an active adaptation of abalone to the light environment over time, which in turn enhances tolerance to environmental stress.

Purines are mainly in the form of purine nucleotides in the body, which play a crucial role in regulating energy supply, metabolic regulation, and the composition of coenzymes [47]. The metabolism of purines largely depends on adenosine deaminase and xanthine oxidase. Of which, adenosine deaminase can catalyze the conversion of adenine nucleoside to hypoxanthine nucleoside, then generate hypoxanthine under the action of nucleoside phosphorylase, until it is finally converted to uric acid by xanthine oxidase [48]. In 6 M vs 14 M and 14 M vs 22 M, the Purine metabolism pathway was significantly enriched and Guanosine 5′-phosphate was significantly down-regulated in 6 M vs 14 M. In contrast, the expression levels in 14 M vs 22 M were significantly upregulated, indicating that the expression levels of Guanosine 5′-phosphate tended to decrease during the day and increase at night. The expression levels of hypoxanthine were significantly upregulated in 6 M vs 14 M, but were significantly downregulated in 14 M vs 22 M, and its expression levels tended to increase during day and decrease at night. Hypoxanthine is a metabolite of nucleosides enables tissues and cells under low-energy, hypoxic state to continue with the metabolism process, stimulate the body to produce antibodies, and enhance immunity [49]. Therefore, the changes in the content of hypoxanthine not only indicate the conversion of energy metabolism of abalone at day and night, but also contribute to enhanced immunity under the light environment.

In conclusion, after continuous monitoring of the circadian behaviours of abalone, the cumulative movement distance and cumulative movement time of abalone were highest between 00:00–03:00 h. Average and maximum crawling speeds were lowest from12:00–15:00 h and 21:00–00:00 h, indicating that the maximum crawling speed of abalone was lower in dark periods, but its crawling distance and movement time were longer. In particular, its ecological habits under the dark environment were consistent with that of its nocturnal ecological habits. Metabolomics analysis identified 380, 385, and 315 metabolites with significant differences in 6 M vs 14 M, 14 M vs 22 M, and 6 M vs 22 M, of which arachidonic acid metabolism was significantly enriched in each comparison group. In contrast, purine metabolism, tryptophan metabolism, and glycerophospholipid metabolism were significantly enriched in 14 M vs 22 M and 6 M vs 14 M. In the transition from light to dark environment, the expression levels of phosphatidylcholine, 5-HT, *N*-acetyl-5-hydroxytryptamine, indole-3-acetaldehyde, hypoxanthine, and deoxyinosine reduced, while those of lysoPC(20:5(5Z,8Z,11Z,14Z,17Z)), lysoPC(22:4(7Z,10Z,13Z,16Z)), lysoPC(16:1(9Z)/0:0), PE(18:1(11Z)/22:2(13Z,16Z)), and guanosine 5′-phosphate rose. These 11 metabolites function as differential metabolic markers which play a critical role in the adaptation of abalone to the alternation of day and night. These findings not only provide a quantitative description of the diurnal movement behaviours of abalone, but also give a preliminary analysis of the physiological and metabolic mechanism of its nocturnal behaviour, and a reference for the optimization of light environment factors and the proper selection of feeding strategies during artificial aquaculture.

Supplementary data to this article can be found online at https://doi.org/10.1016/j.jphotobiol.2020.111994.

Author Contributions

The authors' responsibilities were as follows: X.L. Gao, W.W. You and C.H. Ke conceptualized the study; X.L. Gao conducted research and collected the data; X. Luo provided the materials and interpreted the data; X.L. Gao wrote the manuscript; C.H. Ke had primary responsibility for the final content. All authors read and approved the final manuscript.

Declaration of Competing Interest

The authors declare that they have no known competing financial interests or personal relationships that could have influenced the work reported in this paper.

Acknowledgements

This research was supported by grants from the Chinese Ministry of Science and Technology through the National Key Research and Development Program of China (2018YFD0901400), Fujian Ocean and Fisheries Research Grand (FJHJF-L-2020-7), Earmarked fund for the Modern Agro-industry Technology Research System (CARS-49), China Postdoctoral Science Foundation Grant (2019M650153), and the Outstanding Postdoctoral Scholarship from the State Key Laboratory of Marine Environmental Science at Xiamen University.

References

[1] J.F. Taylor, B.P. North, M.J.R. Porter, N.R. Bromage, H. Migaud, Photoperiod can be used to enhance growth and improve feeding efficiency in farmed rainbow trout, *Oncorhynchus mykiss*, Aquaculture. 256 (2006) 216–234.
[2] T. Wang, Y.Z. Cheng, Z.P. Liu, S.H. Yan, X.H. Long, Effects of light intensity on growth, immune response, plasma cortisol and fatty acid composition of juvenile *Epinephelus coioides* reared in artificial seawater, Aquaculture. 414 (2013) 135–139.
[3] N. Bromage, M. Porter, C. Randall, The environmental regulation of maturation in farmed finfish with special reference to the role of photoperiod and melatonin, Aquaculture. 197 (2001) 63–98.
[4] C. Gentile, H. Sehadova, A. Simoni, C.C. Chen, R. Stanewsky, Cryptochrome antagonizes synchronization of Drosophila's circadian clock to temperature cycles, Curr. Biol. 23 (2013) 185–195.
[5] K.J. Lohmann, C.M.F. Lohmann, N.F. Putman, Magnetic maps in animals: nature's GPS, J. Exp. Biol. 210 (2007) 3697–3705.
[6] A.D. Beale, D. Whitmore, D. Moran, Life in a dark biosphere: a review of circadian physiology in "arrhythmic" environments, J. Comp. Physiol. B. 186 (2016) 947–968.
[7] J.D. Johnston, J.M. Ordovás, F.A. Scheer, F.W. Turek, Circadian rhythms,

metabolism, and chrononutrition in rodents and humans, Adv. Nutr. 7 (2016) 399–406.
[8] G.H. Son, H.K. Cha, S. Chung, K.J. Kim, Multimodal regulation of circadian glucocorticoid rhythm by central and adrenal clocks, J. Endocr. Soc. 2 (2018) 444–459.
[9] E. Challet, Minireview: entrainment of the suprachiasmatic clockwork in diurnal and nocturnal mammals, Endocrinology. 148 (2007) 5648–5655.
[10] S.M. Reppert, A colorful model of the circadian clock, Cell. 124 (2006) 233–236.
[11] X. Yang, A wheel of time: the circadian clock, nuclear receptors, and physiology, Genes Dev. 24 (2010) 741–747.
[12] Food and Agriculture Organization of the United Nations (FAO), Rome, FishStatJ, www.fao.org/fishery/statistics/en, (2019).
[13] R.C. Wang, Z.P. Wang, Science of Marine Shellfish Culture, China Ocean University Press, Qingdao, 2008, pp. 434–435.
[14] Z. Garcia-Esquivel, S. Montes-Magallon, M.A. Gonzalez-Gomez, Effect of temperature and photoperiod on the growth, feed consumption, and biochemical content of juvenile green abalone, *Haliotis fulgens*, fed on a balanced diet, Aquaculture. 262 (2007) 129–141.
[15] E. Gorrostieta-Hurtado, R. Searcy-Bernal, C. Anguiano-Beltrán, Z. García-Esquivel, E. Valenzuela-Espinoza, Effect of darkness on the early postlarval development of *Haliotis corrugata* abalone fed different diatom densities, Cienc. Mar. 35 (2009) 113–122.
[16] F. Ahmed, S. Segawa, M. Yokota, S. Watanabe, Effect of light on oxygen consumption and ammonia excretion in *Haliotis discus discus*, *H. gigantea*, *H. madaka* and their hybrids, Aquaculture. 279 (2008) 160–165.
[17] R. Day, P. Gilmour, S. Huchette, Effects of density and food supply on postlarval abalone: behaviour, growth and mortality, J. Shellfish Res. 23 (2004) 1009–1018.
[18] X.L. Gao, M. Zhang, J.M. Zheng, X. Li, L. Chi, C.B. Song, Y. Liu, Effect of LED light quality on the phototaxis and locomotion behavior of *Haliotis discus hannai*, Aquac. Res. 47 (2015) 3376–3389.
[19] X.L. Gao, M. Zhang, X. Li, F.C. Wu, Y. Liu, Light cycle effects on *Haliotis discus hannai* Ino growth, energy budget, and related gene expression, Aquaculture. 483 (2018) 213–222.
[20] W.A. Hoogerwerf, H.L. Hellmich, G. Cornélissen, F. Halberg, V.B. Shahinian, J. Bostwick, T.C. Savidge, V.M. Cassone, Clock gene expression in the murine gastrointestinal tract: endogenous rhythmicity and effects of a feeding regimen, Gastroenterology. 133 (2007) 1250–1260.
[21] P. Domenici, The scaling of locomotor performance in predator-prey encounters: from fish to killer whales, Comp. Biochem. Phys. A. 131 (2001) 169–182.
[22] M. Almbro, C. Kullberg, Impaired escape flight ability in butterflies due to low flight muscle ratio prior to hibernation, J. Exp. Biol. 211 (2008) 24–28.
[23] J. Weber, The physiology of long-distance migration: extending the limits of endurance metabolism, J. Exp. Biol. 212 (2009) 593–597.
[24] S.A. Shepherd, Movement of the Southern Australian abalone *Haliotis laevigata* in relation to crevice abundance, Australian J. Ecol 11 (2006) 295–302.
[25] L.E. Morgan, L.W. Botsford, S.R. Wing, B.D. Smith, Spatial variability in growth and mortality of the red sea urchin, *Strongylocentrotus franciscanus*, in northern California, Can. J. Fish. Aquat. Sci. 57 (2000) 980–992.
[26] M.D. Kintzing, M.J. Butler, The influence of shelter, conspecifics, and threat of predation on the behavior of the long-spined sea urchin (*Diadema antillarum*), J. Shellfish Res. 33 (2014) 781–785.
[27] E.G. Day, G.M. Branch, Influences of the sea urchin *Parechinus angulosus* (Leske) on the feeding behaviour and activity rhythms of juveniles of the south African abalone *Haliotis midae* Linn, J. Exp. Mar. Biol. Ecol. 276 (2002) 1–17.
[28] G.C. Dong, S.L. Dong, F. Wang, X.L. Tian, Effects of materials, incubation time and colors of artificial shelters on behavior of juvenile sea cucumber *Apostichopus japonicas*, Aquac. Eng. 43 (2010) 1–5.
[29] A. Mercier, S.C. Battaglene, J.-F. Hamel, Daily burrowing cycle and feeding activity of juvenile sea cucumbers *Holothuria scabra* in response to environmental factors, J. Exp. Mar. Biol. Ecol. 239 (1999) 125–156.
[30] J.-F. Hamel, A. Mercier, Diet and feeding behaviour of the sea cucumber *Cucumaria frondosa* in the St. Lawrence estuary, eastern Canada, Can. J. Zool. 76 (1998) 1194–1198.
[31] R. Goodacre, S. Vaidyanathan, W.B. Dunn, G.G. Harrigan, D.B. Kell, Metabolomics by numbers: acquiring and understanding global metabolite data, Trends Biotechnol. 22 (2004) 245–252.
[32] A. Anwar-Mohamed, O.H. Elshenawy, A.A. El-Sherbeni, M. Abdelrady, A.O. El-Kadi, Acute arsenic treatment alters arachidonic acid and its associated metabolite levels in the brain of C57Bl/6 mice, Can. J. Physiol. Pharmacol. 92 (2014) 693–702.
[33] Q.F. Zhu, Y.H. Hao, M.Z. Liu, J. Yue, J. Ni, B.F. Yuan, Y.Q. Feng, Analysis of cytochrome P450 metabolites of arachidonic acid by stable isotope probe labeling coupled with ultra high-performance liquid chromatography/mass spectrometry, J. Chromatogr. A 1410 (2015) 154–163.
[34] J. Bellien, C. Fréguin-Bouilland, R. Joannidès, M. Hanoy, I. Rémy-Jouet, C. Monteil, M. Iacob, et al., High-efficiency on-line haemodiafiltration improves conduit artery endothelial function compared with high-flux haemodialysis in end-stage renal disease patients, Nephrol. Dial. Transplant. 29 (2014) 414–422.
[35] C. Zhou, J. Huang, Q. Li, C. Zhan, X. Xu, X. Zhang, D. Ai, et al., CYP2J2-derived EETs attenuated ethanol-induced myocardial dysfunction through inducing autophagy and reducing apoptosis, Free. Radical. Bio. Med. 117 (2018) 168–179.
[36] M.C. Gong, A. Fuglsang, D. Alessi, S. Kobayashi, P. Cohen, A.V. Somlyo, A.P. Somlyo, Arachidonic acid inhibits myosin light chain phosphatase and sensitizes smooth muscle to calcium, J. Biol. Chem. 267 (1992) 21492–21498.
[37] S. Saha, A.A. Anilkumar, S. Mayor, GPI-anchored protein organization and dynamics at the cell surface, J. Lipid Res. 57 (2016) 159–175.
[38] N.D. Ridgway, The role of phosphatidylcholine and choline metabolites to cell proliferation and survival, Crit. Rev. Biochem. Mol. Biol. 48 (2013) 20–38.
[39] T.D. Heden, P.D. Neufer, K. Funai, Looking beyond structure: membrane phospholipids of skeletal muscle mitochondria, Trends Endocrinol. Metab. 27 (2016) 553–562.
[40] K. Funai, I.J. Lodhi, L.D. Spears, L. Yin, H. Song, S. Klein, C.F. Semenkovich, Skeletal muscle phospholipid metabolism regulates insulin sensitivity and contractile function, Diabetes. 65 (2016) 358–370.
[41] A. Selathurai, G.M. Kowalski, M.L. Burch, P. Sepulveda, S. Risis, R.S. Lee-Young, S. Lamon, et al., The CDP-ethanolamine pathway regulates skeletal muscle diacylglycerol content and mitochondrial biogenesis without altering insulin sensitivity, Cell Metab. 21 (2015) 718–730.
[42] R. Wu, Z. Wu, X. Wang, P. Yang, D. Yu, C. Zhao, G. Xu, et al., Metabolomic analysis reveals that carnitines are key regulatory metabolites in phase transition of the locusts, P. Natl. Acad. Sci. USA. 109 (2012) 3259–3263.
[43] K. Schröcksnadel, B. Wirleitner, C. Winkler, D. Fuchs, Monitoring tryptophan metabolism in chronic immune activation, Clin. Chim. Acta 364 (2006) 82–90.
[44] V. Carcangiu, C. Giannetto, S. Luridiana, G. Piccione, Features of the daily rhythms of blood melatonin and glucose in goats during different natural photoperiod, Chronobiol. Int. 35 (2017) 1–7.
[45] N. Farhadi, M. Gharghani, Z. Farhadi, Effects of long-term light, darkness and oral administration of melatonin on serum levels of melatonin, Biom. J. 39 (2016) 81–84.
[46] A.T. Slominski, R. Hardeland, M.A. Zmijewski, R.M. Slominski, R.J. Reiter, R. Paus, Melatonin: a cutaneous perspective on its production, metabolism, and functions, J. Invest. Dermatol. 138 (2018) 490–499.
[47] Z.H. Su, H.M. Jia, H.W. Zhang, Y.F. Feng, L. An, Z.M. Zou, Hippocampus and serum metabolomic studies to explore the regulation of Chaihu-Shu-Gan-san on metabolic network disturbances of rats exposed to chronic variable stress, Mol. BioSyst. 10 (2014) 549–561.
[48] N. Dalbeth, L. Stamp, Hyperuricaemia and gout: time for a new staging system, Ann. Rheum. Dis. 73 (2014) 1598–1600.
[49] R. Harrison, Structure and function of xanthine oxidoreductase: where are we now? Free Radic. Biol. Med. 33 (2002) 774–797.